# Resolution of a paradox: Hummingbird flight at high elevation does not come without a cost

**Douglas L. Altshuler*†, Robert Dudley*‡, and Jimmy A. McGuire‡§**

*Section of Integrative Biology, University of Texas, Austin, TX 78712; ‡Department of Integrative Biology, University of California, Berkeley, CA 94720; and §Museum of Natural Science, Louisiana State University, Baton Rouge, LA 70803

Edited by David B. Wake, University of California, Berkeley, CA, and approved October 12, 2004 (received for review July 20, 2004)

**Flight at high elevation is energetically demanding because of parallel reductions in air density and oxygen availability. The hovering flight of hummingbirds is one of the most energetically expensive forms of animal locomotion, but hummingbirds are nonetheless abundant at high elevations throughout the Americas. Two mechanisms enhance aerodynamic performance in high-elevation hummingbirds: increase in wing size and wing stroke amplitude during hovering. How do these changes in morphology, kinematics, and physical properties of air combine to influence the aerodynamic power requirements of flight across elevations? Here, we present data on the flight performance of 43 Andean hummingbird species as well as a 76-taxon multilocus molecular phylogeny that served as the historical framework for comparative analyses. Along a 4,000-m elevational transect, hummingbird body mass increased systematically, placing further aerodynamic demands on high-elevation taxa. However, we found that the minimum power requirements for hovering flight remain constant with respect to elevation because hummingbirds compensate sufficiently through increases in wing size and stroke amplitude. Thus, high-elevation hummingbirds are not limited in their capacity for hovering flight despite the challenges imposed by hypobaric environments. Other flight modes including vertical ascent and fast forward flight are more mechanically and energetically demanding, and we accordingly also tested for the maximum power available to hummingbirds by using a load-lifting assay. In contrast to hovering, excess power availability decreased substantially across elevations, thereby reducing the biomechanical potential for more complex flight such as competitive and escape maneuvers.**

animal flight | aerodynamic power requirements | hummingbird phylogeny

Hummingbirds are the only vertebrates capable of sustained hovering, a highly strenuous form of locomotion requiring extraordinary levels of metabolic power input (1) and mechanical power output (2). Because oxygen availability and air density decrease at higher elevations, hovering flight in alpine habitats is particularly challenging. From an aerodynamic perspective, it is therefore surprising that hummingbirds are most diverse in the Andes and reach elevations as high as 5,000 m (3, 4).

Body mass, wing size and shape, wingbeat frequency, and wing stroke amplitude are important morphological and biomechanical parameters underlying hovering flight performance (5), and are likely to be the targets of selection along an elevational gradient (6). Because mass-specific induced power requirements in hovering flight are proportional to the square root of wing loading (5), high-elevation hummingbirds would benefit aerodynamically by being smaller and by having larger wings relative to low-elevation taxa. Aerodynamic theory also predicts that the mass-specific induced power requirements of hovering are inversely proportional to the square root of stroke amplitude (5). Thus, increase in this kinematic parameter should yield significant reduction in hovering costs. Available data are largely consistent with these aerodynamic predictions. Among taxa, hummingbirds compensate for reduced air density at high elevations by having larger wings relative to their body mass (6, 7). Further increases in lift are accomplished by increased stroke amplitudes, which have been demonstrated experimentally through reductions in air density and comparatively across elevations (8, 9). Each of these compensatory mechanisms will also influence the aerodynamic power requirements for flight, and thus the total power available for flight maneuvers beyond that required for hovering or slow forward flight.

Here, we present data on hummingbird morphology and flight mechanics for 43 hummingbird species distributed along a 4,000-m elevational gradient in the Peruvian Andes. In conjunction with this biomechanical field study, we also present a multilocus phylogenetic data set and analysis that served as the historical framework for the comparative analysis of flight performance and elevational data. The field data consist of morphological parameters related to power requirements of flight and flight kinematics derived from video films of two flight modes: (*i*) free-flight hovering was used to calculate the minimum aerodynamic power requirements for flight; and (*ii*) flight during maximal load-lifting was used to calculate the maximum aerodynamic power that hummingbirds could produce (10). Comparing maximum power production for load-lifting to minimum power requirements for hovering yields the power margin, which is a measure of the excess aerodynamic power that is available for more energetically demanding flight modes such as vertical ascent (11) and fast forward flight (12).

## Methods

**Phylogenetic Analysis.** We collected 3,114 aligned base pairs of DNA sequence data representing two nuclear [$\beta$ fibrinogen intron 7 (Bfib) and adenylate kinase intron 5 (AK1)] and one complete mitochondrial gene (ND2) for 75 species of hummingbirds and one outgroup taxon (the chimney swift, *Chaetura pelagica*). Our ingroup sampling included a broad selection of hummingbird lineages representing all previously identified major groupings. Complete methodology for DNA purification, amplification, and sequencing is available in supporting information, which is published on the PNAS web site. (for additional details, see refs. 13–15). DNA sequences are available from GenBank (accession nos. AY830455–AY830681).

DNA alignments were performed initially by using CLUSTALW and later modified by eye. MACCLADE 4.06 (16) was used to verify that ND2 protein coding gene sequence remained in frame throughout its length. A number of indels in the AK1 and BFib sequences could not be aligned with confidence and were consequently excluded from further analysis.

We performed a Bayesian phylogenetic analysis by using a parallel implementation of MRBAYES version 3.04b (17). We used

This paper was submitted directly (Track II) to the PNAS office.

Data deposition: The sequences reported in this paper have been deposited in the GenBank database (accession nos. AY830455–AY830681).

†To whom correspondence should be sent at the present address: California Institute of Technology, Mail Code 138-78, 1200 East California Boulevard, Pasadena, CA 91125. E-mail: doug@caltech.edu.

**Table 1. Description of field sites in southeast Peru including the elevation (m), partial pressure of oxygen ($P_{O_2}$), air density ($\rho$), and the number of taxa captured**

| Site name | Elevation, m | $P_{O_2}$, mmHg | $\rho$, kg/m$^3$ | No. of taxa |
|---|---|---|---|---|
| Pantiacolla | 400 | 152.05 | 1.17 | 13 |
| Amazonia | 500 | 150.31 | 1.16 | 19 |
| San Pedro | 1,480 | 133.95 | 1.03 | 11 |
| Union | 1,800 | 129.04 | 0.99 | 3 |
| Pillahuata | 2,650 | 116.24 | 0.90 | 15 |
| Huacarpay | 3,090 | 110.32 | 0.85 | 4 |
| Acjanaco | 3,450 | 104.95 | 0.81 | 2 |
| Canchayoc | 3,650 | 102.45 | 0.79 | 7 |
| Cachimayo | 3,665 | 102.26 | 0.79 | 4 |
| Huancarani | 3,860 | 99.05 | 0.76 | 3 |
| Abra Malagra | 4,300 | 93.83 | 0.72 | 2 |

1 mmHg = 133 Pa.

a fully partitioned GTR + Invariant sites + Γ model of DNA substitution with five designated data partitions: ND2 first codon positions, ND2 second codon positions, ND2 third codon positions, BFib, and AK1. Five independent Markov chain Monte Carlo analyses were each run for 15 million generations. After termination of the independent analyses, we first identified and discarded those sample points that were collected before convergence of the chains. We used two strategies to confirm that the chains had achieved stationarity. First, we produced "burn-in" plots by plotting log-likelihood scores as well as all model parameter values against generation number. All sample points obtained before the achievement of a stable equilibrium were then treated as part of the "burn-in" sample and were discarded before the generation of a consensus phylogram with mean branch length estimates and posterior probability values for each node. Second, we used cumulative and sliding window analyses of posterior probability scores to verify that these values were stable across all post-burn-in generations within each analysis by using the application CONVERGE (18). Posterior probability values are not expected to vary directionally (either upward or downward) over time once the Markov chain has achieved stationarity, and substantial deviations from an equilibrium value over time would suggest that the chain had not yet converged.

We also used several methods to ensure that our analyses did not become trapped on local optima. First, we used metropolis-coupled Markov chain Monte Carlo with each of our five independent analyses including a cold chain and three incrementally heated chains (19). When heated chains are included in an analysis, the magnitude of difference between two likelihood scores is compressed relative to the difference that would be observed if the chain is unheated. Thus, a suboptimal topology or suite of parameter values is more likely to be accepted in the context of a heated chain as opposed to the cold chain, thereby allowing heated chains greater opportunity to cross valleys separating local optima on a complex likelihood surface. Second, we compared the burn-in plots, topologies, and posterior probability values obtained across each of the five independent analyses, each of which was initiated from random starting points and confirmed that each achieved very similar outcomes (19).

**Morphology, Kinematics, and Aerodynamic Power.** Data were collected at 11 sites in the Departments of Cusco and Madre de Dios in southeastern Peru, which spanned an elevational range from 400 to 4,300 m (Table 1). Hummingbirds were captured in mist nets and then measured and filmed before being released. Body mass was determined to within 0.001 g by using an Acculab (Edgewood, NY) digital scale (model no. PP-2060D) or to within 0.1 g by using a hanging spring balance (Avinet, Dryden, NY). We took digital photographs of each wing against a background of graph paper, which was used as the scale in subsequent analyses. Wing length was measured from the wing outline, and span-wise wing chord lengths were then determined at 1-pixel intervals along the wing length. Total wing area is the sum of the areas of each wing stripe, defined as the wing chord (in mm) multiplied by the width (in mm) of each pixel. Nondimensional moments of wing area were calculated by using equations in ref. 20. Muscle and wing masses were either measured or calculated from regressions of measured masses with body mass (6).

We filmed hummingbirds during free hovering and while lifting the maximum weight possible. During load-lifting trials, a rubber harness connected to a beaded and color-coded thread was placed over the head of each hummingbird. The hummingbirds were released on the floor of a small flight chamber (0.9 m high by 0.45 m wide by 0.45 m long). Because the natural escape response of a hummingbird is to fly directly up and toward light, as birds attempted escape they lifted progressively more beaded weights until they reached maximum sustained load. The typical behavior of a hummingbird in load-lifting is to fly as high as possible, and then to hover briefly before descending laterally toward the chamber wall (10, 11). One camera (Sony Video 8 CCD-TR44) filmed a mirror held at 45° above the flight chamber to attain horizontal wing projections and flight kinematics. Horizontal projection of wing motions yield accurate wing stroke amplitudes because the stroke plane angle of hummingbird wings is close to zero (21, 22). A second camera (Sony Video 8XR CCD-TRV16) was synchronized to the first camera by setting internal clocks. It filmed the floor of the chamber to determine the number of remaining beads, and thus by subtraction, the total weight sustained vertically by the bird.

The maximum weight lifted by each hummingbird was identified, and up to three lifting flight sequences were analyzed if available. Wingbeat kinematics during both maximal load-lifting and free flight were determined by using frame-by-frame analysis of films. Wingbeat frequency was determined by using the interaction frequency between the wingbeat frequency and the filming rate (60 frames per sec) of the video film (8, 9). Stroke amplitude was determined from angular wing positions at the maximum forward and backward positions of a wingbeat. The kinematic values for each of the maximum lifts for individual hummingbirds were then averaged.

Physical properties of air at each site and the morphological and kinematic variables of hummingbirds were used to calculate the aerodynamic power output for flight (5). We used an empirically derived profile drag coefficient measured from a revolving hummingbird wing, and bracketed our aerodynamic power estimates by assuming either high (0.469) or low (0.139) profile drag coefficients ($C_{D,pro}$) corresponding to high (45°) and low (15°) angles of attack of the wing (23). The maximum power available to hummingbirds was calculated as the power margin: the ratio of the maximum power produced during load-lifting to the minimum power required for steady hovering. Morphological, kinematic, and power data were averaged for each gender of each species. The species mean is the average of the values for the two genders. All comparative data were analyzed by using least squares regression. In addition to analyses of raw species data, phylogenetic similarity among these data were corrected for by calculating standardized independent contrasts (24). In these cases, regressions were constrained to go through the origin (25).

## Results

**Phylogenetics.** Each of the five independent Bayesian analyses conducted here appeared to have converged within ≈500,000 generations. Nevertheless, to be conservative, we discarded the

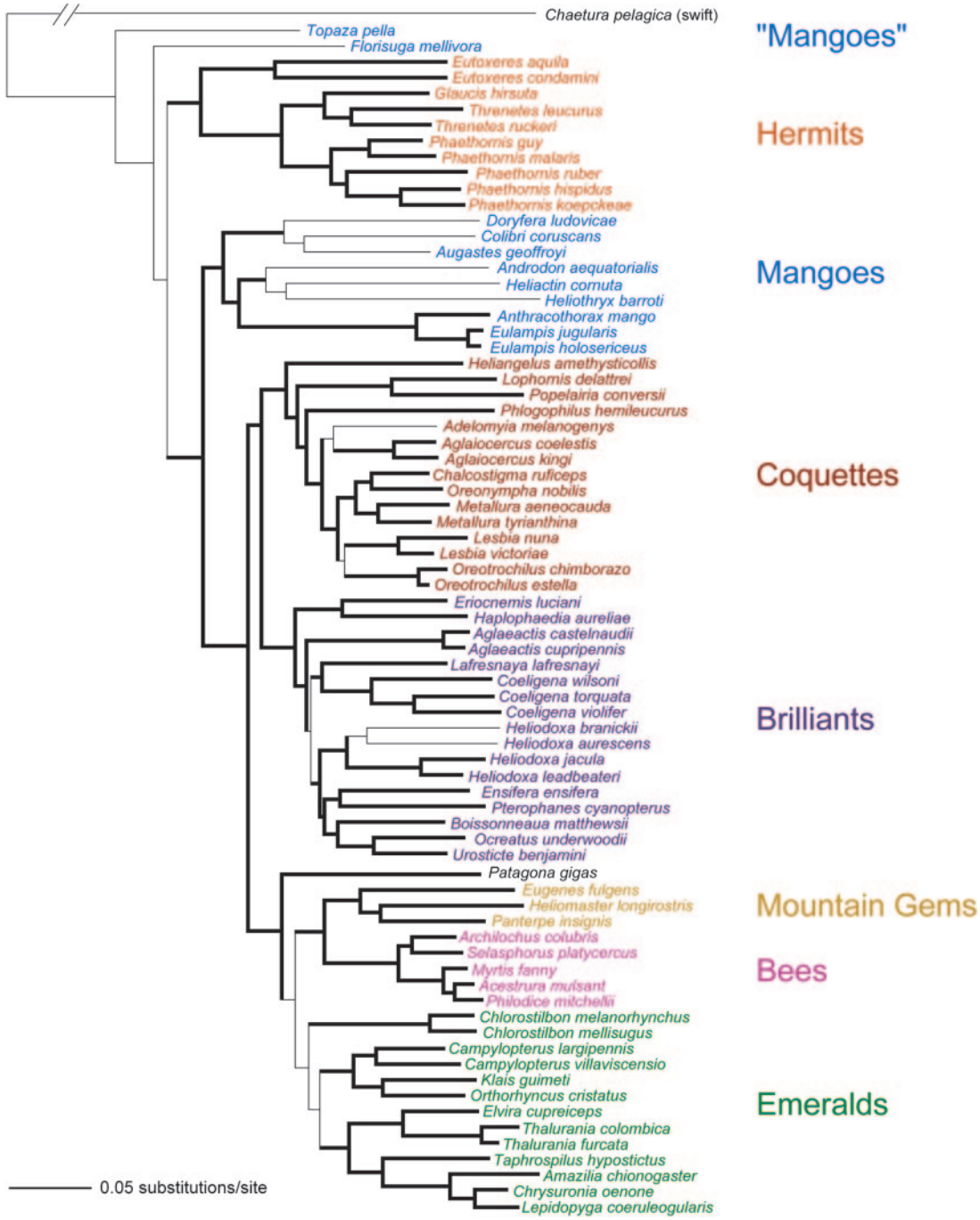


**Fig. 1.** Phylogenetic estimate of hummingbird relationships. Heavy lines represent nodes with posterior probability values of 95% or greater. Informal suprageneric groupings are based on Bleiweiss *et al.* (26) and/or suggested relationships in the Handbook of Birds of the World (28). Taxonomy follows that of Sibley and Monroe (44), except for the treatments of *Phaethornis* (45) and *Heliodoxa* (46). The branch representing the giant hummingbird, *Patagona gigas*, is not color-coded because it is not definitively aligned with a specific suprageneric group.

first 2 million generations of each analysis as burn-in. Recovered topologies and posterior probability values were highly correlated across the five independent analyses, again indicating that the chains had converged. The data corresponding to the final 13 million generations of each of the five independent analyses were ultimately pooled, allowing a consensus topology with mean branch lengths and posterior probability values to be calculated on the basis of 65,000 sample points (see Fig. 1). Our analysis of two nuclear and one mitochondrial gene for the 75 ingroup taxa resulted in a well supported estimate of hummingbird phylogenetic relationships. Of the 75 nodes on the tree, 62 received posterior probability values >95%, and 53 of 75 received posterior probability values of 100.

**Morphology, Kinematics, and Aerodynamic Power.** Morphological measurements were made for 484 captured individual hummingbirds from 43 species. Flight trials were conducted on most of these individuals, but accurate kinematic data during maximal load lifts were available for only 347 individuals, but with all taxa represented. Of the 43 species, 42 were included in the phylo-

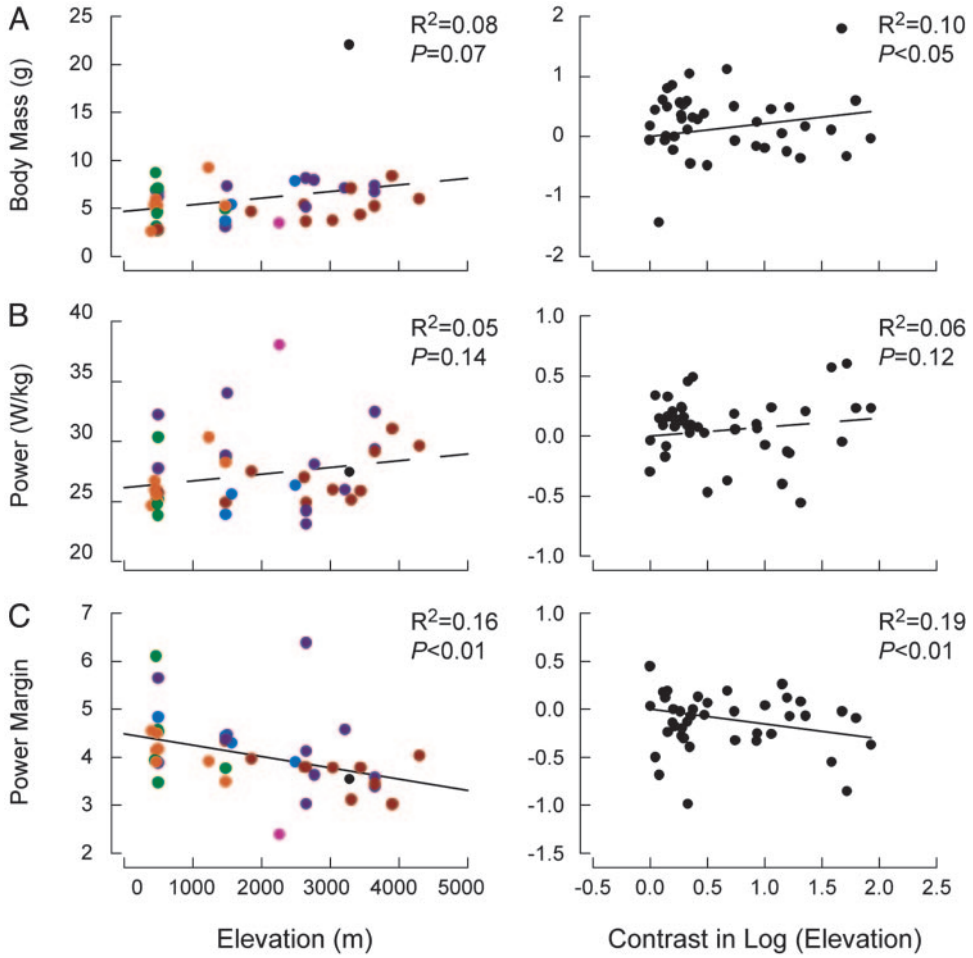


**Fig. 2.** Changes in hummingbird morphology and flight performance with elevation. Raw species data are given at *Left* (color coded to the clades from Fig. 1), and standardized independent contrasts are given at *Right*. Data points represent species means (or their contrasts), and equations for relationships with elevation are given in the figure panels. (*A*) Hummingbird body mass increases with elevation. The outlying point is for the giant hummingbird *P. gigas*. All analyses were performed with and without this taxon, and neither the trends nor the overall significance relationships changed. The depicted values of mechanical power represent aerodynamic (induced plus profile) power calculated per kilogram of body mass, and estimated by using a $C_{D,pro}$ value of 0.139. (*B*) The minimum power requirements for free flight hovering exhibit no significant trend with elevation. (*C*) The power margin decreases across elevations.

genetic estimate, which contained no polytomies (Fig. 1). Thus, 41 ($n - 1$) phylogenetically independent contrasts were available for comparative analyses.

Interspecifically, hummingbird body mass increased slightly with increasing elevation (Fig. 2*A*) possibly as a thermal response to reduction in average environmental temperature. Nonetheless, increased body mass at high elevations adds additional aerodynamic cost because greater lift must be generated to offset body weight. Because body mass changed with elevation, all subsequent regressions are multiple regressions with two independent variables: body mass and elevation.

A complete description of changes in hummingbird wing size and wingbeat kinematics with elevation for the Andean community from southeast Peru has been presented elsewhere (9). In summary, one aerodynamically compensatory mechanism for larger hummingbirds at high elevation is an increase in wing size, although this response would follow isometrically from an increase in body mass. However, hummingbird wings are also relatively larger at high elevations, as indicated by a negative relationship between wing loading (the ratio of body weight to wing area) and elevation (6). Second, high-elevation hummingbird species also compensate for reduced air density by increasing stroke amplitudes (9). Wingbeat frequency, by contrast, is inversely correlated with body mass and exhibited no significant trend with elevation ($P > 0.1$).

The minimum aerodynamic power required for hovering flight was invariant across elevations (Fig. 2*B*) regardless of which profile drag coefficient was used in power calculations. The power margin indicates the extent of excess power available for flight, and exhibited a significant decrease with elevation (Fig. 2*C*) for either estimate of the profile drag coefficient.

## Discussion

Our analysis of hummingbird phylogenetics provides a well supported and well resolved phylogenetic estimate for the group based on reasonably broad sampling. This sequence-based topology is remarkably congruent with the landmark DNA–DNA hybridization tree of Bleiweiss *et al.* (26), but nearly triples the number of represented species from 26 to 75. Our analysis confirms the informal suprageneric taxonomy of Bleiweiss *et al.* (26), which suggests major monophyletic hummingbird assemblages, and we follow these authors in identifying these clades as Hermits, Mangoes, Coquettes, Brilliants, Emeralds, Mountain Gems, and Bees (Fig. 1). However, a few taxa included in the present study cannot be placed objectively within the Bleiweiss *et al.* (26) framework. *Topaza pella* and *Florisuga mellivora* always fall out near the base of the tree and, surprisingly, are often

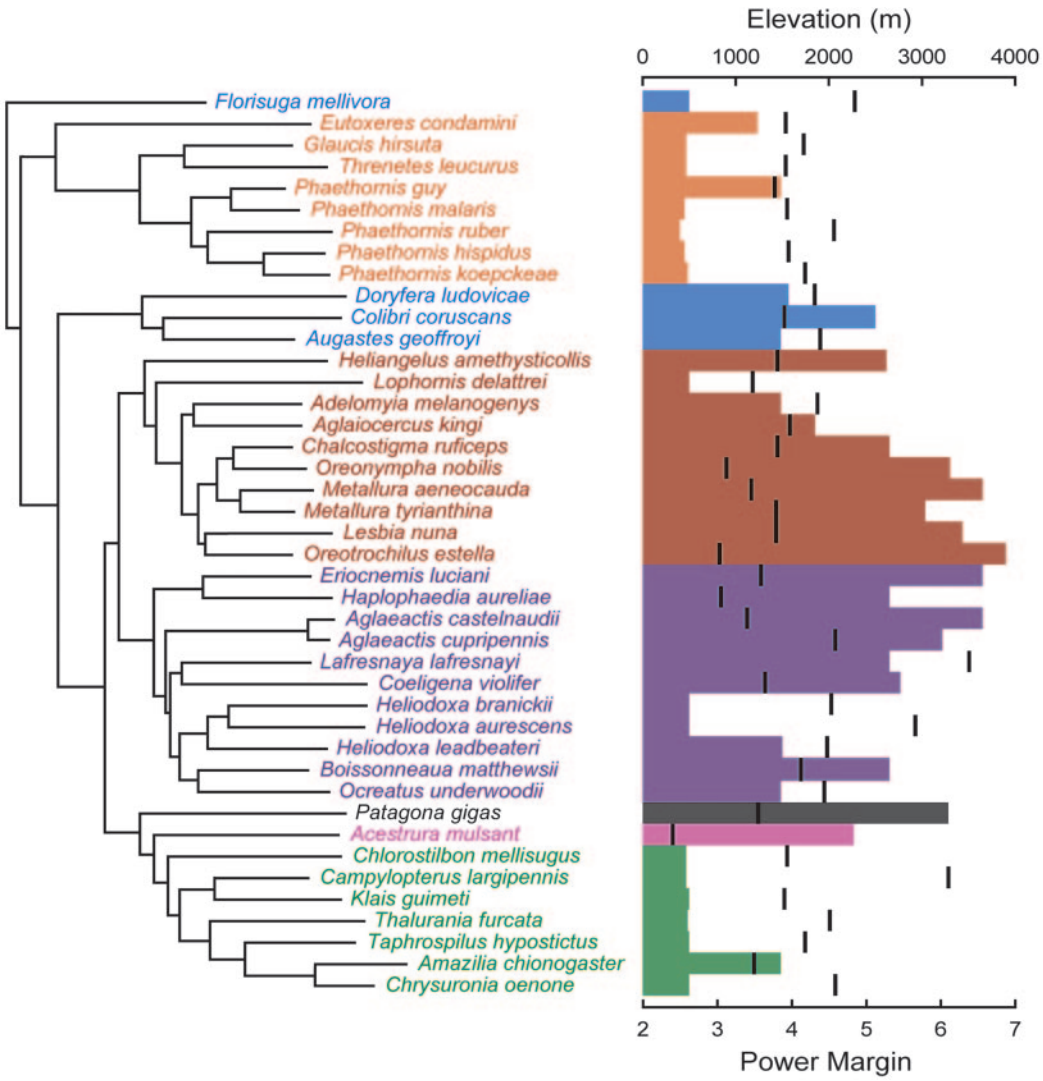


**Fig. 3.** Phylogenetic distribution of power margin (black lines) and elevation (colored bars) for those Andean hummingbirds included in the flight performance study. Many of the high-elevation taxa are from the Brilliant (purple) and Coquette (maroon) clades. Within all clades, hummingbirds at low elevations tend to have higher power margins.

placed basal to Hermits. Also, the giant hummingbird, *P. gigas*, is weakly placed as the sister of a clade comprised of Emeralds, Mountain Gems, and Bees. Because the primary objective of the present paper is related to flight performance, we refrain from addressing these issues in the present paper.

It is widely appreciated that flight in hummingbirds is one of the most energetically expensive forms of vertebrate locomotion (27). Nonetheless, hummingbirds are abundant throughout alpine habitats in the western hemisphere (28), where hypobaric air presents a further challenge. Here, we have investigated how morphological and kinematic changes with elevation influence flight performance. Decreases in wing loading with elevation were first noted by Feinsinger *et al.* (7), who correspondingly predicted that power requirements of hovering were invariant with respect to elevation. The idea that the challenges of flight do not change across elevation contradicts at least some predictions from aerodynamic theory, but our analysis lends strong support to this hypothesis.

Although hummingbirds are highly successful at minimizing the power requirements for hovering flight at low barometric pressures, flight performance is nonetheless compromised with respect to more energetically demanding flight modes. Larger wings at high elevations are clearly compensatory, but also carry the additional aerodynamic cost of reducing wingbeat frequency (29). As further compensation, increases in stroke amplitude with elevation provide additional lift to balance power demands. However, because hummingbirds reach a limit to lifting performance at stroke amplitudes near 180° (8, 9), the compensatory increase in amplitude for hovering at high elevations also limits the magnitude of excess power available. Thus, progressive colonization of high-elevation habitats has not been without cost given the systematic decrease in the power margin (Fig. 3).

In addition to the aerodynamic consequences of hypodense air, other environmental features of high-elevation habitats are likely to influence hummingbird flight performance. We have studied elsewhere the hovering performance of hummingbirds in hypoxia by gradually replacing ambient air with pure nitrogen (9). Because nitrogen has density similar to that of normal air, this experiment tested for effects of hypoxia while maintaining an almost constant air density. Although two species of hummingbirds exhibited adverse responses to hypoxia, the changes were minor and apparent only at concentrations well below those encountered naturally. An external source of energetic compensation could arise through increases in flower or sucrose avail-

ability at high elevation. However, available data from Costa Rica (30) and Mexico (31) indicate that sugar availability actually decreases with elevation. Thus, alpine hummingbirds may be constrained energetically as well as aerodynamically.

We conclude that high-elevation residence by hummingbirds has not compromised hovering performance *per se*. Instead, evolutionary responses in wingbeat kinematics and flight-related morphology have facilitated flight at higher altitudes by larger hummingbird taxa, which may also enjoy competitive thermoregulatory advantage mediated by increased body size. This phylogenetically based analysis of hummingbird flight performance demonstrates substantial evolutionary flexibility in wingbeat kinematics and concomitant aerodynamic power production.

Limits to locomotor performance are also suspected to influence behavior, a hypothesis recently confirmed for several taxa. Experimental studies in lizards and birds have revealed that multiple aspects of maximal performance, including sprint speed (32), aerobic scope (33), and endurance (34), are correlated with dominance behavior. Previous attempts to link hummingbird flight performance and behavior (both competitive ability and nectar foraging) have relied on morphological surrogates for flight capacity (35), but the available data do not support a mechanistic basis to behavior based solely on morphology (36). A more recent experimental study of flight performance and competitive ability in two species of *Selasphorus* hummingbirds indicates that power margins may strongly influence behaviors at high elevations where excess power is limiting (37).

In addition to competitive ability and foraging for both insects and flower nectar, the complex aerial displays that males perform to attract females and advertise territories may also be strongly influenced by flight capacity. These display flights consist of rapid vertical ascents and dives as well as fast horizontal components (38–40), which may be used by females and competing males to evaluate the displaying hummingbird. It would be highly informative to examine the relationship between power margin values and species-specific flight displays to determine whether these advertise male energetic capacity.

Given the importance of aerodynamic power availability to the biogeography and ecology of hummingbirds, we suggest two areas worthy of further investigation. First, hummingbird muscles exhibit numerous adaptations for enhanced performance (41, 42), but little is known regarding how muscle activity is controlled to regulate muscle force production in this group. Second, hummingbirds engage in multiple flight modes besides hovering and are capable of very fast forward flight (43) and remarkable aerial maneuvers, but the relationship between muscle and aerodynamic force production for these behaviorally relevant flight modes remains unclear.

We thank C. Barber, R. Gibbons, and Earthwatch Institute (Maynard, MA) volunteers for assistance with fieldwork in Peru. Additional help was provided by P. Baik, M. Dillon, A. Gilbert, J. Goldbogen, W. Palomino, and V. Yabar. We thank M. Van Vlaardingen and Pantiacolla Tours (Peru), B. Gomez, C. Munn, R. Yabar, and B. Walker for logistical support. This work was supported by National Science Foundation Grants IBN 9817138 and DEB 0330750 and grants from the Earthwatch Institute.

1. Suarez, R. K. (1992) *Experientia* **48,** 565–570.
2. Wells, D. J. (1993) *J. Exp. Biol.* **178,** 39–57.
3. Rahbek, C. & Graves, G. R. (2000) *Proc. R. Soc. London Ser. B* **267,** 2259–2265.
4. Carpenter, F. L. (1976) *Univ. California Publ. Zool.* **106,** 1–74.
5. Ellington, C. P. (1984) *Philos. Trans. R. Soc. London B* **305,** 145–181.
6. Altshuler, D. L. & Dudley, R. (2002) *J. Exp. Biol.* **205,** 2325–2336.
7. Feinsinger, P., Colwell, R. K., Terborgh, J. & Chaplin, S. B. (1979) *Am. Nat.* **113,** 481–497.
8. Chai, P. & Dudley, R. (1995) *Nature* **377,** 722–725.
9. Altshuler, D. L. & Dudley, R. (2003) *J. Exp. Biol.* **206,** 3139–3147.
10. Chai, P., Chen, J. S. C. & Dudley, R. (1997) *J. Exp. Biol.* **200,** 921–929.
11. Chai, P. & Millard, D. (1997) *J. Exp. Biol.* **200,** 2757–2763.
12. Berger, M. (1985) in *BIONA Report 3*, ed. Nachtigall, W. (Gustav Fischer, Stuttgart), pp. 307–314.
13. Prychitko, T. M. & Moore, W. S. (1997) *Mol. Phylogenet. Evol.* **8,** 193–204.
14. Shapiro, L. H. & Dumbacher, J. P. (2001) *Auk* **118,** 248–255.
15. Sorenson, M. D., Ast, J. C., Dimcheff, D. E., Yuri, T. & Mindell, D. P. (1999) *Mol. Phylogenet. Evol.* **12,** 105–114.
16. Maddison, D. R. & Maddison, W. P. (2003) MACCLADE (Sinauer, Sunderland, MA), version 4.
17. Huelsenbeck, J. P. & Ronquist, F. (2001) *Bioinformatics* **17,** 754–755.
18. Warren, D. L., Wilgenbusch, J. & Swofford, D. L. (2003) CONVERGE (University of California, Davis).
19. Huelsenbeck, J. P. & Bollback, J. P. (2001) *Syst. Biol.* **50,** 351–366.
20. Ellington, C. P. (1984) *Philos. Trans. R. Soc. London B* **305,** 17–40.
21. Chai, P. & Dudley, R. (1996) *J. Exp. Biol.* **199,** 2285–2295.
22. Stolpe, V. M. & Zimmer, K. (1939) *J. Ornithol.* **87,** 136–155.
23. Altshuler, D. L., Dudley, R. & Ellington, C. P. (2004) *J. Zool.* **264,** 327–332.
24. Felsenstein, J. (1985) *Am. Nat.* **125,** 1–15.
25. Garland, T., Harvey, P. H. & Ives, A. R. (1992) *Syst. Biol.* **41,** 18–32.
26. Bleiweiss, R., Kirsch, J. A. W. & Matheus, J. C. (1997) *Mol. Biol. Evol.* **4,** 325–343.
27. Suarez, R. K. (1998) *J. Exp. Biol.* **201,** 1065–1072.
28. Schuchmann, K. L. (1999) in *Handbook to the Birds of the World*, eds. del Hoyo, J., Elliott, A. & Sargatal, J. (Lynx Edicions, Barcelona), Vol. 5, pp. 468–680.
29. Greenewalt, C. H. (1962) *Smithsonian Misc. Collections* **144,** 1–46.
30. Hainsworth, F. R. & Wolf, L. L. (1972) *Comp. Biochem. Physiol.* **42,** 359–366.
31. Cruden, R. W., Hermann, S. M. & Peterson, S. (1983) in *The Biology of Nectaries*, eds. Bentey, B. & Elias, T. (Columbia Univ. Press, New York), pp. 80–125.
32. Garland, T., Hankins, E. & Huey, R. B. (1990) *Funct. Ecol.* **4,** 243–250.
33. Hammond, K. A., Chappell, M. A., Cardullo, R. A., Lin, R. S. & Johnsen, T. S. (2000) *J. Exp. Biol.* **203,** 2053–2064.
34. Perry, G., Levering, K., Girard, I. & Garland, T. (2004) *Anim. Behav.* **67,** 37–47.
35. Feinsinger, P. & Chaplin, S. B. (1975) *Am. Nat.* **109,** 217–224.
36. Altshuler, D. L., Stiles, F. G. & Dudley, R. (2004) *Am. Nat.* **163,** 16–25.
37. Altshuler, D. L. (2001) Ph.D. dissertation (University of Texas, Austin), pp. 221.
38. Calder, W. A., Calder, L. L. & Frazier, T. D. (1990) *Experimentia* **46,** 999–1002.
39. Larimer, J. L. & Dudley, R. (1995) *Auk* **112,** 1064–1066.
40. Stiles, F. G. (1982) *Condor* **84,** 208–225.
41. Gaunt, A. S. & Gans, C. (1993) *J. Morphol.* **215,** 65–88.
42. Suarez, R. K., Lighton, J. R. B., Brown, G. S. & Mathieu-Costello, O. (1991) *Proc. Natl. Acad. Sci. USA* **88,** 4870–4873.
43. Chai, P., Altshuler, D. L., Stephens, D. B. & Dillon, M. E. (1999) *Physiol. Biochem. Zool.* **72,** 145–155.
44. Sibley, C. G. & Monroe, B. L. (1990) *Distribution and Taxonomy of Birds of the World* (Yale Univ. Press, New Haven, CT).
45. Hinkelmann, C. & Schuchmann, K. L. (1997) *Studies Neotropical Fauna Environ.* **32,** 142–163.
46. Gerwin, J. A. & Zink, R. M. (1989) *Wilson Bull.* **101,** 525–544.